^{29}Si and ^{27}Al MAS NMR study of the zeolitization of kaolin by alkali leaching

N. BENHARRATS[1],*, M. BELBACHIR[2], A. P. LEGRAND[3] AND
J.-B. D'ESPINOSE DE LA CAILLERIE[3]

[1]*LPPMC, Département de Chimie, Faculté des Sciences, Université des Sciences et Technologie, BP 1505, Al M'nouer Oran 31000, Algeria,* [2]*L.C.P. Département de Chimie, Faculté des Sciences, Université d'Es-Senia, BP 1525, Al M'nouer Oran 31000, Algeria, and* [3]*Systèmes Interfaciaux à l'Echelle Nanométrique, FRE CNRS 2312, Laboratoire de Physique Quantique, Ecole Supérieure de Physique et de Chimie Industrielles de la Ville de Paris, 10 rue Vauquelin 75231, Paris cedex 05, France*

ABSTRACT: The alkali leaching of two aluminosilicates, kaolinite and metakaolinite, with aqueous NaOH has been studied. Both silicates gave hydroxysodalite (HS) with or without the evanescent zeolite NaA. X-ray diffraction and high-resolution ^{29}Si and ^{27}Al MAS-NMR spectroscopy provide information about the reaction sequence of the clay. The conversion starts with the formation of an amorphous gel precursor at a rate which depends on the alkali concentration but not on the choice of kaolinite or metakaolinite as starting material. The rate of zeolitization of this gel is much faster when it is obtained from kaolinite, probably because it is more homogeneous.

Surface chemistry, surface area and surface charge are the most important properties in terms of kaolinite applications. Surface treatment of clays (when they are used as fillers and reinforcements in polymers) is a well-known way to modify the interfacial interaction in composites (Ishida & Kumar, 1978; Ishida, 1988). Non-reactive treatment results in a decrease in the surface tension of the filler leading to an increase in particle/particle and a decrease in particle/polymer interaction (Jones, 1989). Reactive treatment assumes the presence of reactive groups both on the surface of the filler and in the polymer matrix (Todd, 2000).

Kaolinite [$Al_4Si_4O_{10}(OH)_8$], a dioctahedral 1:1 aluminosilicate, is poor in active-OH surface groups which could react with polymers. Nevertheless, it is possible to increase the number and activity of surface OH groups by alkali leaching of kaolinite. Kaolinite is known to give HS on treatment with aqueous alkali at ~100ºC (Barrer, 1982; Engelhardt & Michel, 1987; Madani *et al.*, 1990; MacKenzie *et al.*, 1996). Metakaolinite, obtained by thermal dehydroxylation of kaolinite, is a defect phase in which the tetrahedral silica layers of the original clay structure are largely retained with adjacent AlO_4 tetrahedral units derived from the original octahedral layer (Percival *et al.*, 1974; Lambert *et al.*, 1989). It can be expected to be more reactive than kaolinite as leaching would not be rate limited by the diffusion between the bidimensional layers of a phyllosilicate. Metakaolin has been used for the synthesis of low-silica zeolites such as NaA, NaX and NaY (Breck, 1964).

This paper is an attempt to obtain a better understanding of the effect of alkali leaching at moderate temperature and atmospheric pressure of kaolinite and metakaolinite in view of their potential use as fillers in hydrophilic polymers.

The evolution of reaction products was followed using X-ray diffraction (XRD) and high-resolution [29]Si and [27]Al solid-state Magic Angle Spinning Nuclear Magnetic Resonance (MAS-NMR).

MATERIALS AND METHODS

Materials

Industrial kaolin was kindly supplied by ENOF (Algeria). It comes from Tamazert (eastern Algeria) and is pre-treated into pellets for industrial use through purification with concentrated H_2SO_4, washing, drying and compacting. The chemical compositions of the natural kaolin (UNICER, Spezzano, Italy) and of the acid-treated product (CNRS, Vernaison, France) are reported in Table 1. Metakaolin was obtained from the kaolin by firing at 750°C in a muffle furnace for 8 h. The samples were heated and cooled in air.

10 g of kaolin (K) or metakaolin (MK) were treated separately under stirring with 100 ml of 2 and 6 N NaOH solutions at 80°C in a TPX Erlenmeyer for various reaction times. The reaction products were first centrifuged at 4000 rpm, then filtered in a tubing dialysis membrane (Spectrum Medical Industries, MCWO of 12-14), and washed with distilled water until the pH of the final wash water was approximately 7. Samples were dried at 120°C overnight. The products are denoted as KnNt and MKnNt, n for concentrations of the alkali solutions (2 and 6 N) and t for reaction time in hours.

Methods.

The X-ray diffraction (XRD) patterns were obtained with a Phillips PW 1710 using the Cu-$K\alpha$ line (λ = 1.5418 Å) and operating at 40 kV and 40 mA. The thermal analysis was carried out on a TGA-DTA V1.0B TA Instrument. The specific surface areas of the original and activated samples were determined by the corresponding nitrogen adsorption isotherms at 77 K after outgassing the sample at 120°C for 8 h. The BET method was used for the corresponding calculations.

Magic Angle Spinning Nuclear Magnetic Resonance (MAS-NMR) experiments were performed on Bruker ASX spectrometers using zircon rotors. [27]Al one-pulse experiments were performed at 11.7 T with a spinning rate of 12 kHz, a selective pulse ($<\pi/6$) duration of 0.5 µs, a recycle time 1 s, and 200 acquisitions. The chemical shift was referenced to a 0.1 M aqueous solution of Al(NO$_3$). The [29]Si one-pulse spectra were recorded at 7.04 T with a spinning rate of 4.5 kHz. For one-pulse experiments, the $\pi/2$ pulse duration was 2.5 µs, the recycle time was 5 s, and 500 acquisitions were accumulated. The ^{1}H to [29]Si cross-polarization (CP) pulse scheme was the usual one. The spectra were obtained with a contact pulse (τ) of variable duration, a proton $\pi/2$ pulse width of 5.3 µs, a recycle time of 5 s, and 4000 acquisitions. [29]Si chemical shifts were referenced to TMS.

RESULTS AND DISCUSSION

Thermal analysis and X-ray powder diffraction

The powder XRD data of kaolinite are well known from the literature (Brindley & Brown, 1980) and fully account for the diffraction pattern of the starting kaolin sample, except for the occurrence of quartz at 21°2θ and 27°2θ, and illite at 9°2θ and 18°2θ (Fig. 1). The differential thermal analysis curve is shown in Fig. 2 and is also characteristic of kaolinite. The first endothermic peak at ~90°C corresponds to physisorbed water and the second one at 540°C to dehydroxylation of kaolinite into metakaolinite. At a higher temperature, metakaolinite gives a spinel phase and amorphous SiO_2 at ~975°C and, finally, is transformed into mullite and cristobalite. Also shown in Fig. 2 is the weight loss of this kaolin

TABLE 1. Chemical composition of native (1) and acid-leached kaolin (2).

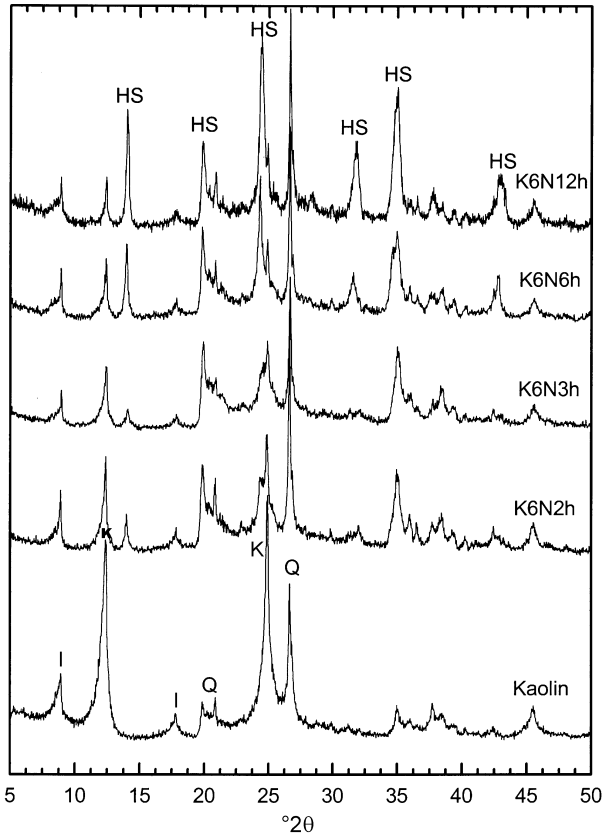| Oxide	SiO$_2$	Al$_2$O$_3$	Fe$_2$O$_3$	FeO	TiO$_2$	CaO	MgO	K$_2$O	MnO	BaO
Wt.% (1)	57.7	37.98	0.96	0.83	0.43	0.54	0.36	1.07	0.04	0.09
Wt.% (2)	48.8	35.5	0.64	0	not analysed					

FIG. 1. XRD patterns of the K6N series with reflections of HS.

as a function of temperature. The BET surface area evolves as a function of calcination temperature. The initial value ($21.4 \ m^2 \ g^{-1}$) is similar to that usually found for kaolinite. In the metakaolin temperature range, the surface area increases by ~20% over that of the original kaolin ($25.8 \ m^2 \ g^{-1}$). Once the kaolin has been heated through the exothermic crystalline transition, the

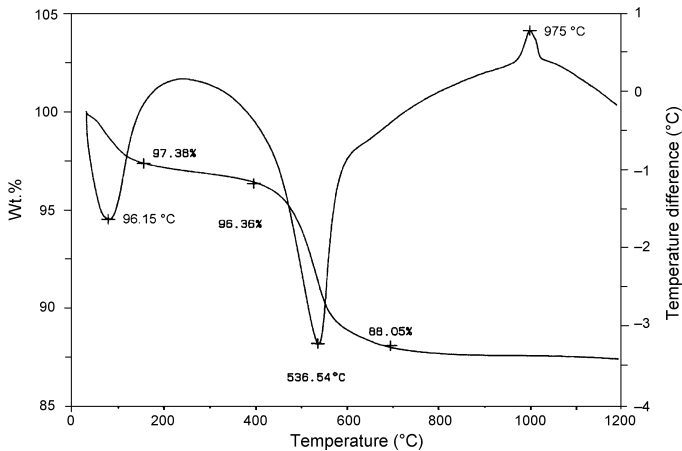FIG. 2. Thermogram of kaolinite.

surface area drops to less than the original value $(16.7 \text{ m}^2 \text{ g}^{-1})$.

Evolution of the solid surfaces resulting from soda activation of the kaolin is given in Table 2. The BET surface area increases with reaction time and with alkali concentrations. Diffraction patterns of the kaolin leached samples for increasing reaction times are represented in Figs 1 and 3. The reflections of kaolinite disappear progressively as the reaction proceeds. For K2N samples, specific lines of NaA zeolite appear after 2 h followed by those for HS after 6 h (Brindley & Brown, 1980). Sample K6N exhibits, after 2 h (Fig. 1), peaks characteristic of HS without the detectable occurrence of NaA. Results of the alkali leaching of the kaolin, as determined by X-ray powder diffraction, are summarized in Table 3.

Metakaolinite is amorphous to X-ray, giving a broad featureless spectrum. The structural changes occurring as the reaction progresses are shown in Figs 4 and 5. The XRD pattern of MK2N shows a

TABLE 2. Specific area of leached samples

Time (h)	K2N $(\text{m}^2 \text{ g}^{-1})$	K6N $(\text{m}^2 \text{ g}^{-1})$
0	21.4	21.4
4	26.7	44.1
6	31.9	51.7
12	39.3	68.3

remarkably different behaviour from that of K2N. No new crystalline phases are observed up to 4 h of reaction time. At 6 h, the only neoformed crystalline phase is the NaA zeolite. For MK6N samples, both HS and NaA are detected simultaneously. Results are summarized in Table 4.

^{27}Al MAS-NMR results

^{27}Al NMR spectra of selected samples from the K and MK series are given in Figs 6 and 7. The

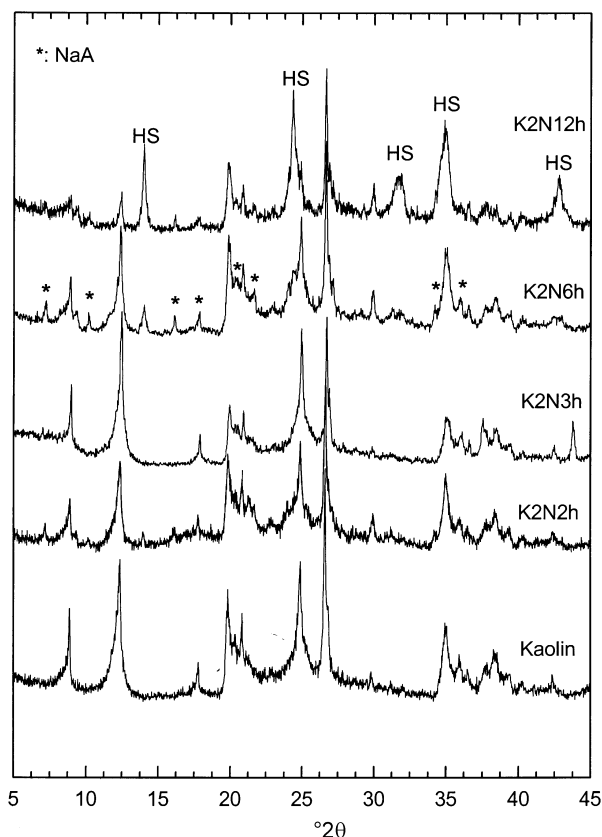

FIG. 3. XRD patterns of the K2N series with reflections of HS and NaA zeolite (*).

TABLE 3. Relative integrated surfaces for ^{29}Si NMR lines and Si/[4]Al ratios for K series. Kaolin samples.

Reaction time	XRD detected phases	91.5 ppm Q^3 (0Al) in kaolinite (%)	−89.5 ppm Q^4 in NaA (%)	−86.5 ppm Q^3(1Al) in kaolinite and Q^4 amorphous and −85 ppm Q^4 in HS (%)
K2N				
0 h	K	89	0	11
2 h	K+NaA	77	8	15
4 h	K+NaA	63	18	19
6 h	K+ NaA+HS	56	21	23
12 h	K+ NaA+HS	31	42	27
K6N				
1 h	K	79		21
2 h	K+HS	71		28
4 h	K+HS	44		55
6 h	K+HS	33		67
12 h	K+HS	11		89

spectrum of the kaolin exhibits mainly the typical resonance at 3 ppm of octahedral aluminium ([6]Al) in a phyllosilicate but also a small but significant (17% of the total intensity) contribution at 70 ppm assigned to aluminium tetrahedrally co-ordinated to oxygen ([4]Al) . The latter shows that the Tamazert kaolin does not consist of pure kaolinite but in fact of an interstratified illite-kaolinite (Yvon, 2000). The [27]Al spectra of K2N samples (Fig. 6) show, in addition to the [4]Al and [6]A1, resonances of the unreacted kaolin, a line at 60 ppm attributed to [5]Al in zeolite (Lippmaa *et al.*, 1986). The maximum of this resonance shifts from 59 to 61 ppm, and its width decreases with increasing reaction time. This reflects structural ordering and

compositional changes from NaA to NaA and HS as observed from XRD. The same spectral features are observed for the K6N series (Fig. 6) except for the line shift. Only HS was detected by XRD.

The ^{27}Al NMR signal of metakaolinite exhibits three lines at 3, 27 and 65 ppm which are typical of [6]Al, aluminium pentacoordinated to oxygen ([5]Al), and [4]Al respectively (Fig. 7) (Lambert *et al.*, 1989). For both MK2N and MK6N samples (Fig. 7), the spectra consist, apart from residual MK resonances, of a resonance at 59 ppm corresponding again to [4]Al in NaA. A shoulder at 61 ppm marking the formation of [5]Al in HS is also observed for the MK6N series, again in good agreement with XRD.

TABLE 4. Relative integrated surfaces for ^{29}Si NMR lines and Si/[4]Al ratios for MK series. Metakaolin samples.

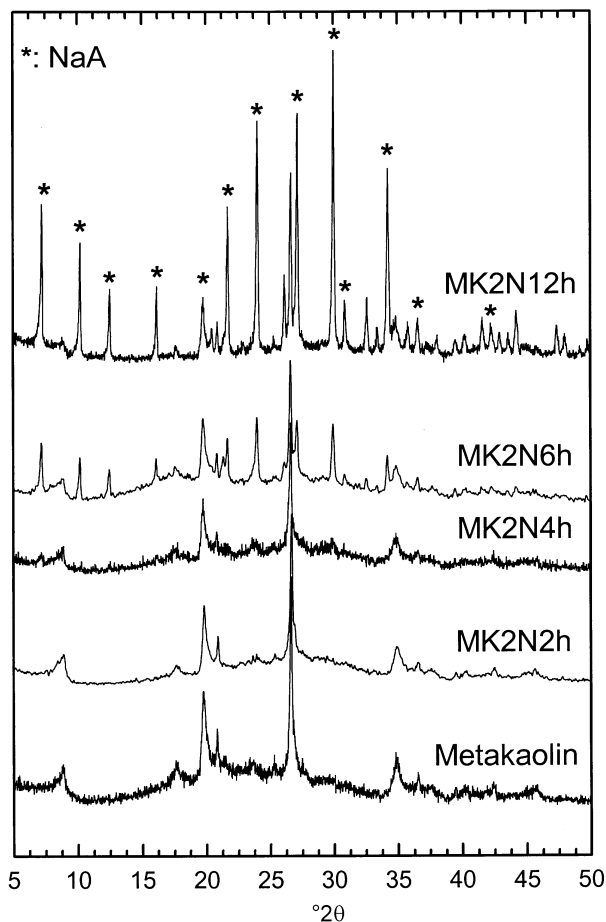| Reaction time	XRD detected phases	−90 ppm Q^4 in metakaolin (%)	−89.5 ppm Q^4 in NaA (%)	−85 ppm/−86.5 Q^4 in HS and amorphous (%)
MK2N				
2 h	MK	65	30	4
4 h	MK	51	42	7
6 h	MK+NaA	39	50	10
12 h	MK+NaA	8.7	73.7	17.6
MK6N				
2 h	MK	59	33	8
4 h	MK+NaA+HS	29	44	27
6 h	MK+NaA+HS	16	40	43
12 h	MK+NaA+HS	14	24	63

FIG. 4. XRD patterns of the MK2N series with reflections of HS and NaA zeolite (*).

Table 5 gives the integrated relative intensities for each line of ^{27}Al NMR spectra for K and MK6N and MK2N treated samples. The contributions of [4]Al in the zeolite products obviously increase with reaction time at the expense of [6]Al in the starting materials. However, the [4]Al resonances are too broad to quantify HS and NaA formations independently. Interestingly, the contribution of the [4]Al in the starting kaolin sample appears constant at 17%.

^{29}Si MAS-NMR results

^{29}Si NMR resonances in aluminosilicates are abundantly documented (Lippmaa *et al.*, 1980, 1981; Sanz & Serratosa, 1984; Engelhardt & Michel, 1987; Sanz *et al.*, 1988; Rees & Sathy, 1993). The spectra of selected samples from the K and MK series are given in Figs 8 and 9. The [29]Si spectrum of kaolinite (Fig. 8) contains a main resonance at −91.5 ppm corresponding to a Q^3(0Al) site with a shoulder at ~−87 ppm which corresponds to a Q^3(1Al) species. This observation is clearly related to the corresponding [27]Al spectrum. Using Lowenstein's rule, we calculate from the relative intensities the average Si/[4]Al ratio in tetrahedral sheets to be 17.

In the [29]Si spectra of kaolinite leached samples, we found the two resonances at −91.5 and −87 ppm (Figs 8 and 11) as for the residual initial kaolin, but the latter becomes more prominent and narrows with a maximum at −86.5 ppm. In the K6N6 spectra, these changes appear earlier and are more pronounced.

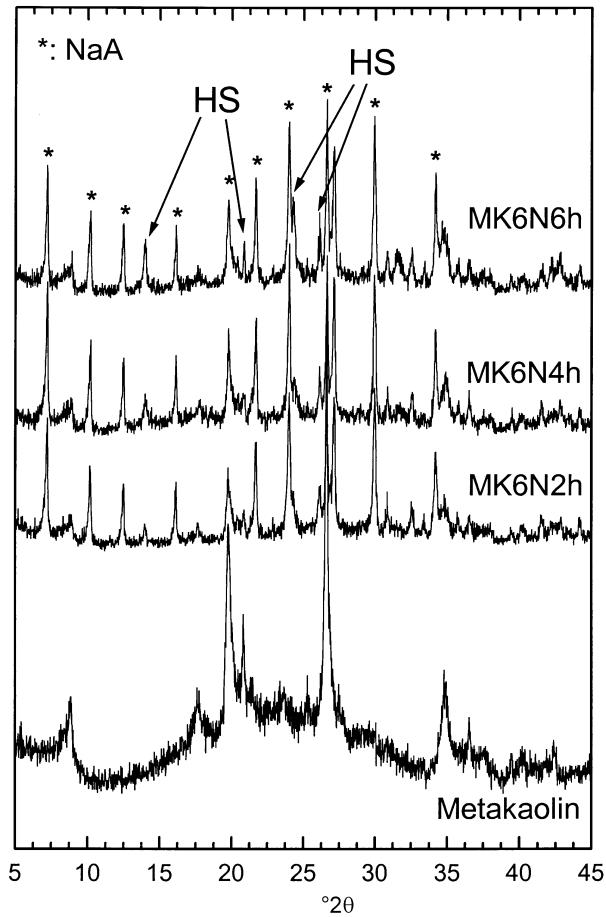^{29}Si NMR spectra of metakaolinite show (Fig. 9) a broad single component, specific to amorphous

FIG. 5. XRD patterns of the MK6N series with reflections of HS and NaA zeolite (*).

materials, centred on −90 ppm. Upon alkali leaching, it splits into two broad resonances at ~−89.5 ppm and −86.5 ppm. As for the kaolinite leached sample, they narrow with reaction time.

TABLE 5. Relative integrated surfaces for ^{27}Al MAS NMR spectra.

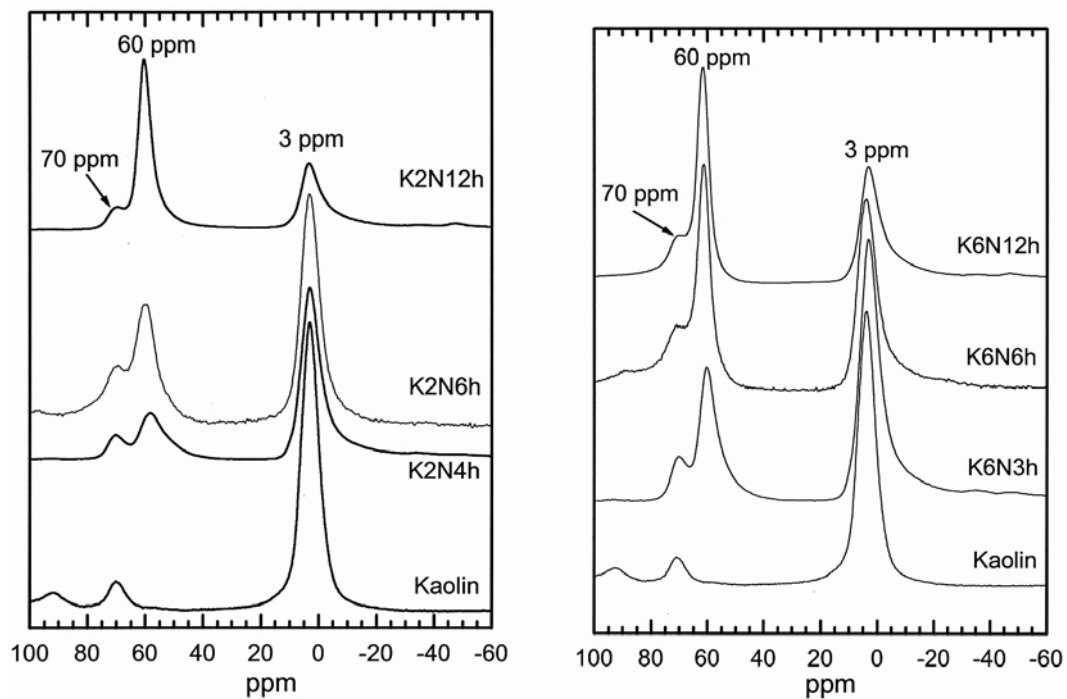| Samples	3 ppm [6]Al (%)	−27 ppm [5]Al in metakaolin (%)	−60 ppm [4]Al in zeolite (%)	70 ppm [4]Al in phyllosilicate (%)
Kaolin	82			18
K2N6h	56		28	17
K2N12h	15		68	17
K6N6h	34		49	17
K6N2h	27		56	17
Metakaolin	52	20		27 (~65 ppm)
MK2N6h	21			79
MK2N2h	7		93	
MKN6h	13		87	
MK6N2h	9		91	

FIG. 6. ^{27}Al NMR spectra of the K2N and K6N series.
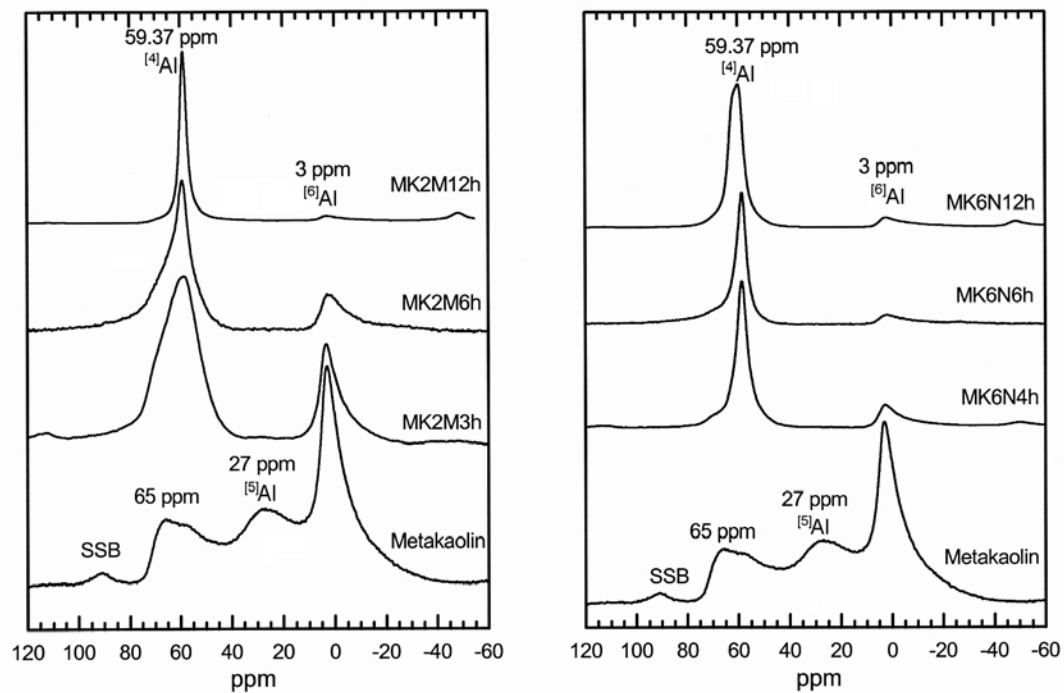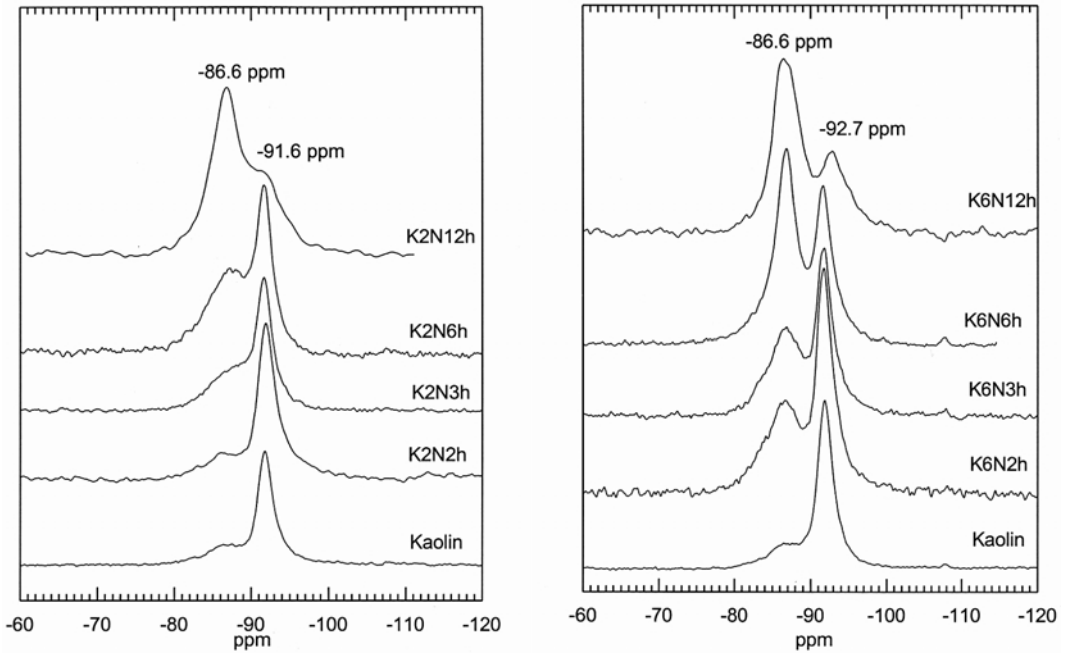

FIG. 7. ^{27}Al NMR spectra of the MK2N and MK6N series.

FIG. 8. One-pulse ^{29}Si NMR spectra of the K2N and K6N leached samples.

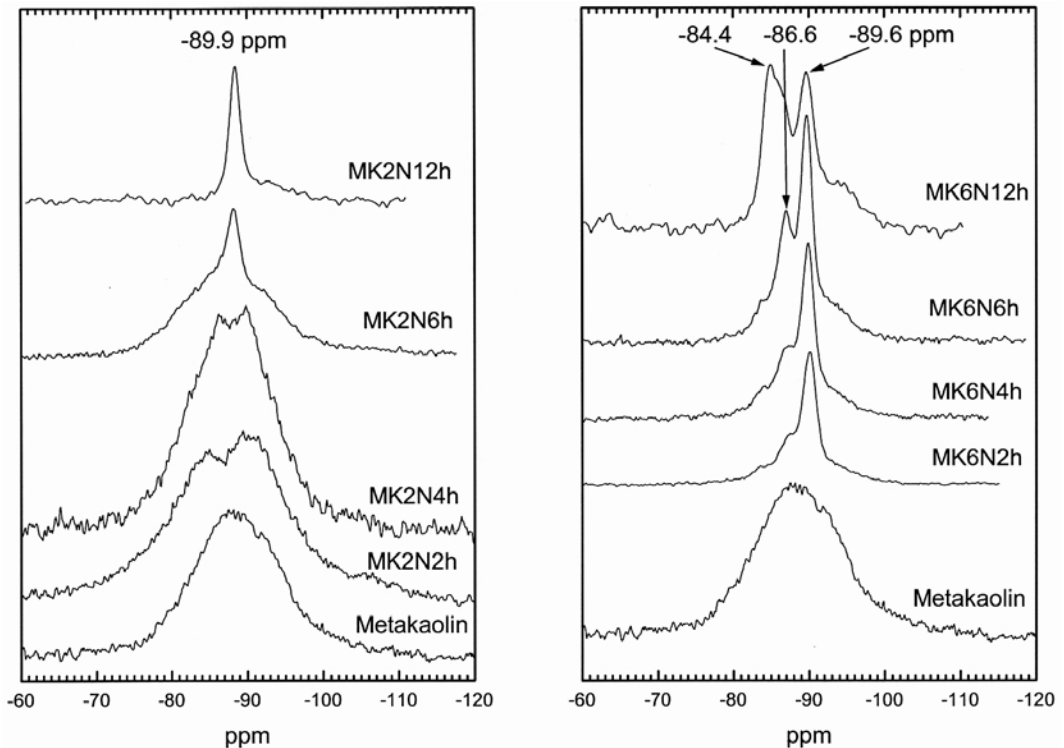FIG. 9. One-pulse ^{29}Si NMR spectra of the MK2N and MK6N series.

Also, the downfield contribution maximum shifts to −85 ppm for the MK6N12 sample.

According to the literature, the resonance at −85 ppm is attributed to a Q^4 site in HS, and that at −89.5 ppm to Q^4 in NaA (Engelhardt & Michel, 1987). In order to fully account for the ^{29}Si NMR spectra, the resonance at −86.5 ppm must be assigned. It could correspond in part to the resonance of $Q^3(1Al)$ sites in residual kaolin but the increase in its intensity upon leaching of metakaolinite, however, cannot be satisfactorily explained in this way. The observed line narrowing is an indication of ordering of the Si environments and reveals that the crystallinity of the reaction products evolves with reaction time. Occurring in the MK samples at 2 h when no crystalline products were detected by XRD, it might, therefore, reflect the formation of an amorphous aluminosilicate phase. $\{^1H\}^{29}Si$ variable contact time CP-MAS experiments were performed to discriminate $Q^3(1Al)$ from an amorphous aluminosilicate Q^4 resonance and confirm this hypothesis.

Cross polarization MAS-NMR results

The CP-MAS NMR spectra of MK series were poorly resolved and did not allow any quantification. The CP-MAS spectra of the feed kaolin exhibit one shift at −91.5 ppm, representative of a $Q^3(0Al)$ environment. At constant contact time between the two spins ^{29}Si-^1H, the kaolinite samples treated for 6 h with 2 N and 6 N concentrations exhibit two features. A distinct line at −91.5 ppm with a shoulder at −86.6 ppm appears clearly in the spectrum (Fig. 10). Interestingly, the relative intensities obtained by integration of the peak surfaces evolve in a different way with respect to the contact time for both the selected samples K6N and K2N when leached for 6 h. Assuming that ^{29}Si are rare compared to ^1H in these aluminosilicates, and that its spin lattice relaxation time in the rotating frame is much longer than the cross polarization time contact, these assumptions are justified in the case of silicates, and it is possible to follow the growth of polarization of the different lines in the CPMAS-NMR spectra with the contact time. The growth of polarization for each separate line can be modelled by (Mehring, 1983):

$$M(\tau) = M_0/\lambda[(1 - \exp(-\tau/T_{Si-H})) \times \exp(-\tau/T_{1\rho H})] \quad (1)$$

with

$$\lambda = [1 - T_{Si-H}/T_{1\rho H}] \quad (2)$$

where T_{Si-H} is the cross polarization time constant responsible for the increase of magnetization, τ is the time of contact of the two spin systems under the Hartman-Hann conditions, $T_{1\rho H}$ is the proton spin lattice relaxation in the rotating frame responsible for the magnetization decay, M is the magnetization and M_0 the magnetization limit. The fitting of the curves gives different values of T_{Si-H} and $T_{1\rho H}$ for the two samples. The $T_{1\rho H}$ values of 7.5 and 9.2 (±0.5) ms are similar for the two lines in the samples K2N and K6N for the resonances at −91.5 and −86.6 ppm, respectively. It was not possible to distinguish between different proton spin reservoirs because of spin exchange. The line at −91.5 ppm has a T_{Si-H} value of 1.2 ±0.1 ms for both K2N6 and K6N6 samples. However, the T_{Si-H} value increases by a factor of 5 between the two samples for the resonance at −86.6 ppm, 1.1 and 5 ms respectively.

The ^{27}Al spectra showed that the intensity of $^{[4]}Al$ phyllosilicate site peaks is constant during the course of the alkali leaching. However, because ^{27}Al in different sites might not provide a
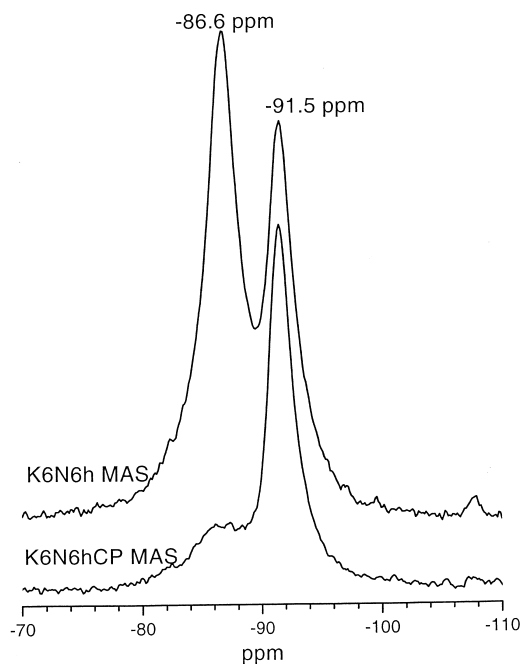

FIG. 10. Superposition of ^{29}Si MAS and ^1H-^{29}Si CP-MAS NMR spectra of the K6N6 sample.

quantitative NMR response due to different quadrupolar effects, this amount cannot be determined directly from the proportion of the [4]Al phyllosilicate resonance in the spectra (17%). Nevertheless, it can be estimated from the ^{29}Si (for which $I = 1/2$, therefore yielding no quadrupolar effects) data. A constant number of [4]Al phyllosilicate sites corresponds to a constant number of $Q^3(1Al)$ sites, and, therefore a constant contribution of those sites to the ^{29}Si NMR response. From the spectrum of the original kaolin, this contribution is taken to be 11%. If this is correct, in the K2N6 sample, about half of the -6.5 ppm contribution (23%) results from the unresolved $Q^3(1Al)$ resonance. Conversely, this resonance contributes only to a sixth of the -86.5 ppm line of the K6N6 (67%). This line is thus in part due to another Si species. This reasonable hypothesis is proved by the CP-MAS T_{Si-H} measurements. Due mainly to a $Q^3(1Al)$ species in the K2N6 sample, the -86.5 ppm resonance exhibits the same rapid polarization transfer (i.e. the same strong coupling to protons) as the other phyllosilicate $Q^3(0Al)$ resonance. In the K6N6 sample, it is due only to a small extent to a Q^3 species, and its T_{Si-H} is much longer. In summary, the analysis of the $\{^1H\}^{29}$Si CP-MAS dynamics proved that the -86.5 ppm resonance results from the unresolved contributions of $Q^3(1Al)$ sites in the unreacted kaolin and from another Si species. ^{27}Al NMR showed the amount of $Q^3(1Al)$ sites to be constant, and it is estimated from one-pulse ^{29}Si NMR to account for 11% of the ^{29}Si spectra. Finally, comparison of XRD and ^{29}Si NMR established that the other Si species must be a Q^4 in an amorphous silicoaluminate.

DISCUSSION

The relative contributions of the HS and NaA zeolites can be obtained through the decomposition of the spectra into Lorentzian components. The relative intensities of each line are given in Tables 3 and 5. However, because the -85, -86.5 and -87 ppm resonances are too close to be separated, only the sum of the three contributions is given. Nevertheless, the Q^4 fraction, not including NaA in the K samples, can be obtained by subtracting the constant (11%) contribution of the $Q^3(1Al)$ sites from the unresolved ^{29}Si resonances between -85 and -86.5 ppm. Such a correction is, of course, not necessary for the MK

series. The Q^4 fractions (not including NaA after correction as explained), relative to the total surface, are plotted against the reaction time in Fig. 11. This plot represents the rate of transformation of the kaolin or the metakaolin into the zeolite HS and its amorphous gel precursor. It appears to be linear with respect to time. This is a clear indication that the zeolitization process is not diffusion limited. Moreover, the rate of reaction, as reflected by the slope, increases with NaOH concentration. No clear difference can be seen between the rate of transformation of kaolin and metakaolin. In order to distinguish the formation of HS from one of the amorphous precursors, the XRD data were also quantified for the 6 N samples (the 2 N samples did not contain enough HS to allow reliable quantifications). The yield of the synthesis of HS was estimated by employing a quantitative analysis based on the peak summation procedure. Accordingly, the areas under the most intense HS peaks at 24, 43, 35 and 32º2θ, corresponding to the crystallographic planes (211), (110), (330) and (310) respectively, were evaluated using the
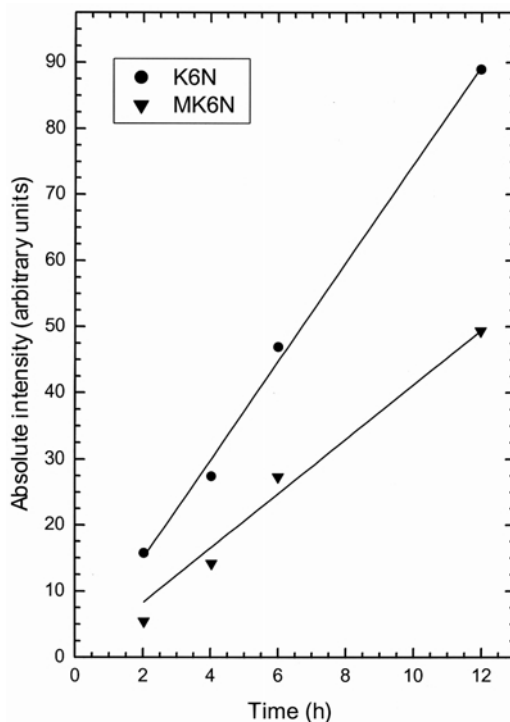

FIG. 11. Plot of HS *vs.* reaction time obtained by XRD as explained in the text: (●) K6N and (▼)MK6N. Lines of slope 7.5 and 4 are drawn.

Philips PC-APD analytical software and summed to each other. Figure 12 shows the evolution of the fraction of HS with time in arbitrary units. As for the NMR data, a linear behaviour is observed but the HS forms faster from the kaolin than from the metakaolin.

Comparison of the qualitative kinetics data obtained from NMR and XRD, therefore, leads to the following conclusion: if one includes the amorphous products, the metakaolin precursor does react as fast as the kaolin, although the HS forms faster for the latter. This shows that the limiting step is not the formation of the amorphous gel precursor but its reorganization into a crystalline HS product. Furthermore, it appears that this reorganization is easier for the gel formed from kaolinite than from metakaolinite. Indeed, although they are likely to have the same composition, they might differ at the molecular scale. In kaolinite, all silicon tetrahedra are co-ordinated to 3 Si and 1 Al through oxygen bridges. In metakaolinite, most of the Si have also 3 Si and 1 Al in their second
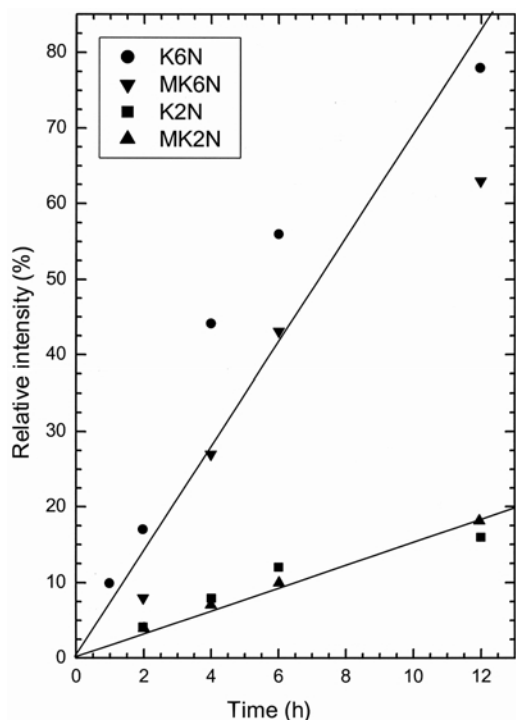
co-ordination sphere but it has been shown that ~5% are in Q^4(0Al) environments (Lambert *et al.*, 1989). The resulting gel is therefore probably more heterogeneous than that resulting from kaolinite, and the time necessary for its reorganization into HS, the induction period, is longer.

CONCLUSIONS

After activation by alkali leaching over several hours, large amounts of kaolinite or metakaolinite remain together with the three reaction products: an amorphous aluminosilicate gel precursor, evanescent zeolite NaA and the final product zeolite HS. For both kaolinite and metakaolinite, conversion is greater at higher alkali concentrations. However, because the reaction is not diffusion limited, the same rate of conversion is observed irrespective of the choice of kaolinite or metakaolinite, i.e. although the ordered structure of kaolinite might hinder the diffusion of active ions from the solid to the aqueous medium, this step is not limiting. Furthermore, with respect to HS formation, kaolinite is more favourable as it forms an amorphous gel precursor that crystallizes more easily into zeolites. With different reaction times and concentrations of alkali, and by first dehydroxylating the kaolin into metakaolin, it is thus possible to prepare samples of varying degrees of zeolitization. We will study their properties, especially with respect to the relative amount of zeolite and amorphous gel and with respect to their use as fillers in polymers like PMMA, POE and other plastics.

FIG. 12. Plot of the relative amount of (HS and amorphous aluminosilicate gel) *vs.* reaction time obtained by NMR as explained in the text: (●) K6N, (▼) MK6N, (■) K2N, (▲) MK2N. Lines of slope 7 and 1.5 are drawn.

REFERENCES

Barrer R.M. (1982) *Hydrothermal Chemistry of Zeolites.* Pp. 153−159. Academic Press, London.

Breck D.W. (1964) Zeolite Molecular Sieve-Structure. Pp. 313−320, 731, 738 in: *Chemistry and Uses.* Wiley, New York.

Brindley G.W. & Brown G., editors (1980) *Crystal Structures of Clay Minerals and their X-ray Identification.* Pp. 495−497. Monograph **5**, Mineralogical Society, London.

Engelhardt G. & Michel D. (1987) *High Resolution Solid State NMR Study of Silicates and Zeolites*. Pp. 205−330. J.Wiley & Sons, NewYork.

Ishida H. (1988) *Interfaces in Polymer, Ceramic and Metal Matrix Composites*. Pp. 101−108. Elsevier, New York.

Ishida H. & Kumar G. (1978) *Molecular Characterization of Composite Interfaces*. Pp. 121−127. Plenum, New York.

Jones F.R. (1989) *Interfacial Phenomena in Composite Materials*. Pp. 141−148. Butterworths, London.

Lambert W., Millman S. & Fripiat J.J. (1989) Revisiting kaolinite dehydroxylation, a ^{29}Si and ^{27}Al MAS NMR study. *Journal of the American Chemical Society*, **111**, 3517−3522.

Lippmaa E., Magi M., Samoson A., Engelhardt G. & Grimer A.R. (1980) Structural studies of silicates by solid-state high resolution ^{29}Si NMR spectroscopy. *Journal of the American Chemical Society*, **102**, 4889−4893.

Lippmaa E., Magi M., Samoson A., Engelhardt G. & Tarmak M. (1981) Investigation of the structure of zeolite by solid state high resolution ^{29}Si NMR spectroscopy. *Journal of the American Chemical Society*, **103**, 4992−4996.

Lippmaa E., Samoson A. & Magi M. (1986) High resolution ^{27}Al NMR of aluminosilicates. *Journal of the American Chemical Society*, **108**, 1730−1735.

MacKenzie K.J.D., Meinhold K.R.H., Chakravorty A.K. & Dafadar M.H. (1996) Thermal reactions of alkali-leached aluminosilicates studied by XRD and solid-state ^{27}Al, ^{29}Si and ^{23}Na MAS NMR. *Journal of Materials Chemistry*, **6**, 833−841.

Madani A., Aznar A., Sanz J. & Serratosa J.M. (1990) ^{29}Si and ^{27}Al NMR study of zeolite formation from alkali-leached kaolinites. Influence of thermal pre-activation. *Journal of Physical Chemistry*, **94**, 760−765.

Mehring M. (1983) *Principles of High Resolution NMR in Solids*, 2nd edition. Pp. 143−155. Springer-Verlag, Berlin.

Percival H.J., Duncan J.F. & Foster P.K (1974) Interpretation of the kaolinite-mullite reaction sequence from Infrared Absorption Spectra. *Journal the American Ceramic Society*, **57**, 57−61.

Rees L.V.C. & Sathy C. (1993) Formation of zeolite from the system Na_2O-Al_2O_3-SiO_2-H_2O in alkaline medium (pH>10). *Zeolites*, **13**, 524−533.

Sanz J. & Serratosa J.M. (1984) [29]Si and ^{27}Al high-resolution MAS NMR spectra of phyllosilicates. *Journal of the American Chemical Society*, **106**, 4790−4793.

Sanz J., Madani A. & Serratosa J.M. (1988) Aluminium-27 and Silicon-29 Magic Angle Spinning Nuclear Magnetic Resonance study of the kaolinite−mullite transformation. *Journal of the American Ceramic Society*, **71**, 418−421.

Todd D.B. (2000) Improving incorporation of fillers in plastics. A special report. *Advances in Polymer Technology*, **19**, 54−59.

Yvon J. (2000) *Les kaolins d'El Mila, amélioration des qualités des kaolins*. Report to ENOF. Laboratoire Environnement et Minéralurgie, INPL Nancy, France.